



PROFESSOR JIAN ZHANG (Orcid ID : 0000-0002-6558-791X)

Article type : Research Article

Design, Synthesis, and Biological Evaluation of Thieno[3,2-d]pyrimidine Derivatives as Potential Simplified Phosphatidylinositol 3-Kinase alpha (PI3K α) inhibitors

Xiuyan Yang^{a,||}, Meng Deng^{a,||}, Xi Zhang^{b,||}, Kun Song^a, Ruan Cong^a, Linghua Meng^{b,*},
Jian Zhang^{a,c,*}

^a Department of Pathophysiology, Key Laboratory of Cell Differentiation and Apoptosis of Chinese Ministry of Education, Shanghai JiaoTong University, School of Medicine, Shanghai 200025, China

^b Division of Anti-tumor Pharmacology, State Key Laboratory of Drug Research, Shanghai Institute of Materia Medica, Chinese Academy of Sciences, Shanghai 201203, China

^c Basic Clinical Research Center, Renji Hospital, Shanghai Jiao Tong University School of Medicine, Shanghai, 200127, China.

* Correspondence to: Jian Zhang (Phone: +86-21-63846590-776922; Fax: +86-21-64154900; Email: jian.zhang@sjtu.edu.cn) or Linghua Meng (Email: lhmeng@simm.ac.cn)

^{||} X. Yang, M. Deng, and X. Zhang contributed equally to this work.

Abstract

A series of thieno[3,2-d]pyrimidine derivatives as phosphatidylinositol 3-kinase (PI3K) inhibitors was designed using the combination strategy. The synthesis and biological evaluation of the derivatives demonstrated their potent inhibition of PI3K, culminating in the discovery of **7** and **21**. Determination of a co-crystal structure of **7** complexed with PI3K α provided the structural basis for the high enzymatic activity. Furthermore, cellular investigation of compounds **7** and **21** revealed that they efficiently suppressed cancer cell lines proliferation through inhibition of intracellular PI3K/AKT/mTOR pathway. The results provided potent simplified inhibitors of PI3K with a promising overall profile and a chemical series for further optimization to progress into vivo experiments.

This article has been accepted for publication and undergone full peer review but has not been through the copyediting, typesetting, pagination and proofreading process, which may lead to differences between this version and the Version of Record. Please cite this article as doi: 10.1111/cbdd.13425

This article is protected by copyright. All rights reserved.

Keywords: PI3K α inhibitors, thieno[3,2-d]pyrimidine derivatives, proliferation inhibition

Running head: Discovery of Potent PI3K α inhibitors

Introduction

The phosphatidylinositol 3-kinase (PI3K)/AKT/mammalian target of rapamycin (mTOR) signaling pathway plays crucial roles in fundamental cellular processes, such as cell growth, survival, migration, and metabolism¹. Aberrant activation of the PI3K/AKT/ mTOR pathway has been associated with many human cancer types^{2,3}. The activation begins with class IA PI3Ks, which can phosphorylate phosphatidylinositol 4,5-bisphosphate (PIP₂) to phosphatidylinositol 3,4,5-trisphosphate (PIP₃). PIP₃ recruits AKT to the membrane and then AKT is phosphorylated at Ser473 by mTOR, which increases its kinase activity and leads to enhance cell survival and growth. This process is negatively regulated by the well-studied tumor suppressor PTEN, which converts PIP₃ back into PIP₂ as a phosphatase⁴⁻⁸. As this critical role in cancer development, PI3K and mTOR have been identified as a tumor-specific drug target. Multiple categories of small molecule inhibitors have recently been reported, including isoform-specific PI3K inhibitor, pan-PI3K inhibitor, ATP competitive mTOR inhibitor, allosteric mTOR inhibitor and PI3K/mTOR dual inhibitor⁹⁻¹⁴. A number of these are currently undergoing clinical trials such as GSK2126458 (GlaxoSmithKline), XL-765 (Exelixis), GDC-0941 (Genentech), and BEZ235 (Novartis) (Figure 1)¹⁵⁻¹⁹.

Our previously complex structure of PI3K α -**9d** revealed that the amino-substituted phenol moiety of **9d** induced conformational change of the Lys802 side chain in the PI3K α , which led to an additional space at the catalytic site for further modification of more potent inhibitors against PI3K α based on compound **9d**²⁰. Meanwhile, studies on analogues of GDC-0941 have shown that thieno[3,2-d]pyrimidine backbone could be explored as replacement for pyrido[3',2':4,5]furo-pyrimidine to simplify the structure of PI3K inhibitors^{21, 22}. So we adopted the combination principle by attaching the amino-substituted phenol moiety of **9d** to a simple thieno[3,2-d] pyrimidine backbone of GDC-0941 to discover a series of thieno[3,2-d]pyrimidine derivatives with low molecular weight (Figure 2). We also modified the substituents at 3-position and 5-position of the phenyl ring and further explored the structure-activity relationship (SAR). The synthesis and biological evaluation of the derivatives demonstrated their potent inhibition of PI3K. Of the 15 tested compounds, compound **7** showed comparable bioactivity against PI3K α with IC₅₀ value of 31.6 \pm 9.4 nM and compound **21** displayed better inhibitory potency against PI3K α with IC₅₀ value of 12.5 \pm 2.8 nM compared to PI103. Moreover, determination of co-crystal structure of PI3K α -**7** illustrated molecular interactions and established the structural basis for further optimization. Finally, the effect of inhibitors **7** and **21** was measured on

SKOV3 and Rh30 cell lines, shown to efficiently suppress proliferation through inhibition of intracellular PI3K phosphorylation.

Material and Method

1. Chemistry

The general synthetic routes used to prepare thieno[3,2-d]pyrimidine derivatives are outlined in the following schemes.

In Scheme 1, commercially available **4** reacted with morpholine in methanol to produce key intermediate **5** according to a similar method reported previously²³. Then, **5** was treated with (3-hydroxy-5-nitrophenyl)boronic acid under Suzuki conditions to provide **6**²⁴. Reduction of **6** with iron powder and aqueous acidified ethanol gave the corresponding aniline **7**. Treatment of **7** with the different aldehyde using standard reductive amination conditions provided the desired derivatives **8-11**. To prepare the 3-fluoro derivate **13**, key intermediate **5** was treated with (3-fluoro-5-nitrophenyl)boronic acid under Suzuki conditions to provide **12**. Reduction of **12** with iron powder and aqueous acidified ethanol provided the desired compound **13**.

Scheme 2 described the route used for the preparation of thieno[3,2-d]pyrimidine derivatives **20-24**. Palladium mediated treatment of 3-bromo-5-hydroxybenzaldehyde **14** with bis(pinacolato)diboron yielded 3-hydroxy-5-(4,4,5,5-tetramethyl-1,3,2-dioxaborolan-2-yl) benzaldehyde **15**. Reaction of **15** with **5** under Suzuki conditions yielded **16**. Acetylation with acetyl chloride resulted in **17**. Reduction of **17** with sodium borohydride yielded **18**. Halogenation of **18** with N-bromosuccinimide (NBS) yielded compound **19**. Finally, **19** was converted into the desired compound **20** by alkaline hydrolysis with 1N NaOH. 3-hydroxy-5-(4-morpholinothieno[3,2-d]pyrimidin-2-yl) benzaldehyde **16**, which was a more versatile intermediate for the preparation of thieno[3,2-d]pyrimidine derivatives, was reacted with a series of different substrates, affording the final derivatives **21-24**.

2. Protein Preparation and Crystallization

To generate human wild-type full-length p110 α and the nSH2 and iSH2 domains (hereafter termed “niSH2”) of p85 α that would be suitable for crystallography, a fusion protein of 6*his-TEV-p85 α (318-615)-linker-p110 α was expressed in the Bac-to-Bac Baculovirus expression system (Invitrogen) using a construct containing the iSH2 domain (467–568) of p85 α fused at the N-terminus of the full-length p110 α , as described previously.¹⁰ To produce a stoichiometric complex to enhance crystallization, analogous niSH2–p110 fusion constructs were designed, incorporating an additional linker between the iSH2 domain and the p110 α in place of the thrombin cleavage site, which is prone to non-specific proteolytic cleavage and accompanying heterogeneity. Using this method, a high purity

of the 6*his-TEV-p85 α (318-615)-linker-p110 α homogeneous fusion protein was obtained via Ni-NTA, Sepharose Q and gel filtration²⁵⁻²⁷. The resulting complex contained all five p110 α domains [an amino-terminal adaptor-binding domain (ABD), residues 1 to 108; a Ras-binding domain (RBD), residues 190 to 291; a C2 (protein-kinase-C homology-2) domain, residues 330 to 480; a helical domain, residues 525 to 696; and a carboxyl-terminal kinase domain, residues 697 to 1068], as well as the nSH2 (residues 318 to 430) and iSH2 (residues 431 to 615) domains of p85 α . Through a sparse matrix screening of 1400 conditions and seeding optimization, a diffraction-quality crystal was produced for data collection²⁸, and an apo crystal was also incubated with 10 mM 7. Diffraction data to a resolution of 2.97 Å were obtained for the 7-p110 α ²⁰.

3. In vitro PI3K Kinase Assays

PI3K inhibitors were dissolved as stock solutions at 10 mM in 100% dimethylsulfoxide (DMSO) and stored in aliquots at -20 °C. The compounds were diluted to the desired concentrations immediately before each experiment. The kinase activity of the purified PI3Ks was determined by the PI3-Kinase Homogeneous Time-Resolved Fluorescence Assay (HTRF Assay) (Millipore). The assays were performed according to the manufacturer's protocol. Briefly, the EC₈₀ concentration of each enzyme was incubated in the assay buffer, containing 10 μ M PIP₂, in a white 384-well plate (Perkin Elmer). After incubation at room temperature for 30 min, the reaction was initiated by adding ATP and then terminated by adding the stop solution and the detection mix. The final concentrations of ATP were 5 μ M, 20 μ M, 50 μ M, and 20 μ M for p110 α , β , δ and γ , respectively. The plate was then sealed and incubated at room temperature overnight²⁹. The intensity of the light emission was measured by an EnVision Multilabel Reader (PerkinElmer) in TR-FRET mode (excitation at 320 nm and emission at 665 nm)³⁰. The IC₅₀ values were calculated by fitting data to a logistic curve using GraphPad Prism 6 software³¹.

4. Cell Proliferation Assay

The human prostate cancer PC-3 cells were obtained from the American Type Culture Collection (Manassas, VA) and maintained in Ham's F-12 medium (Invitrogen, Carlsbad, CA). The human ovarian cancer SKOV3 cells were obtained from the Japanese Foundation of Cancer Research (Tokyo, Japan) and maintained in Dulbecco's modified Eagle's medium (Invitrogen). The Rhabdomyosarcoma Rh30 cells were from St. Jude Children's Hospital (Memphis, TN) and were maintained in RPMI medium 1640 (Invitrogen) with HEPES (10 mM, pH 7.4). All the media were supplemented with 10% FBS (Invitrogen), penicillin (100 IU/ml) and streptomycin (100 μ g/ml). All cells were cultured in a humidified atmosphere of 95% air and 5% CO₂ at 37 °C³².

Cell proliferation was evaluated by a Sulforhodamine B (Sigma-Aldrich) assay as described previously^{12, 33}. In brief, cells seeded in 96-well plates were treated with test compounds in triplicate for 72 h³⁴. The OD value was measured at 560 nM with a multiwell spectrophotometer (VersaMax), and the IC₅₀ values were determined by a four-parameter logit method of the curve-fitting program from SoftMax Pro Software (version 5.4.1, Molecular Devices, Menlo Park, CA)^{20, 35}.

5. Western Blot Analysis

Cells seeded in a twelve-well plate were exposed to the test compounds at the desired concentrations for 1 h. Cells were harvested and subjected to standard Western blot analysis using antibodies against phosphorylated AKT at Ser473 and total AKT (Cell signaling Technology). β -actin (Sigma-Aldrich) was used as a loading control^{20, 35}.

Results and Discussion

1.1. Inhibition of PI3K α activity and SAR

All newly prepared thieno[3,2-d]pyrimidine derivatives were assessed in vitro in terms of biological activity against the PI3K α isoform by using the PI3-Kinase HTRF Assay. PI103 was assigned as positive controls (Table 1).

Using the combination strategy, we successfully obtained the simplified compound **7**, which showed comparable bioactivity against PI3K α to PI103 with IC₅₀ value of 31.6 \pm 9.4 nM. With the long-chain substituted amino-group, **8**, **9**, **10**, and **11** all showed significant loss in activity. The depression of activity became gradually significant with the carbon chain being lengthened and was about 31-fold (IC₅₀ = 0.99 \pm 0.2 μ M), 51-fold (IC₅₀ = 1.6 \pm 0.3 μ M), 128-fold (IC₅₀ = 4.1 \pm 0.8 μ M) and 316-fold (IC₅₀ > 10 μ M) compared to **7**. This data illustrated the long substituent in amino-group could hardly accommodate into the induced pocket and optimization of the chain length was critical to enzymatic activity.

Thus, we began our optimization of the amino-group from **7** with shorter substituents. Replacement of the amino group of **7** with a (*E*)-hydrazonomethyl group or a (*E*)-carboxyvinyl group resulted in **24** (IC₅₀ > 1 μ M) or **23** (IC₅₀ > 1 μ M), which apparently reduced the enzymatic activity. In contrast, the bromomethyl and (*E*)-(hydroxyimino) methyl derivatives, **20** (IC₅₀ = 61.9 \pm 1.1 nM) and **22** (IC₅₀ = 59.2 \pm 9.0 nM) regained its activity, suggesting that the induced pocket only could accommodate smaller substituents. Further optimization with the hydroxymethyl group resulted to the most potent compound **21**, which was about 3-fold more potent than **7**. However, introducing a nitro-group or a formyl group on the phenol group yielded **6** (IC₅₀ = 2.7 \pm 0.8 μ M) and **16** (IC₅₀ > 1 μ M), which was > 31-fold less potent than **7**. These data suggested again importance of the chain length and hydroxymethyl proved to be the optimal length for enzymatic activity.

In a next step, we explored the influence of the hydroxyl group at the R₁ position and found that the fluoro-substitution derivative **13** (IC₅₀ = 6.3 ± 0.1 μM) and acetyl-substituted derivative **19** (IC₅₀ > 1 μM) showed a distinct decrease in potency. It suggested that the hydroxyl group was critical for activity. We speculated that there was a hydrogen bond between the hydroxyl group and its nearby residue located at the binding pocket of PI3K α .

1.2. Crystal Structure of **7** bound to PI3K α

To gain structural insights for the high binding affinity, we attempted to determine co-crystal structure for **7** in a complex with PI3K α . The data collection and refinement statistics were summarized in Table 2. As shown in Figure 3A, the crystal structure of PI3K α -**7** verified that compound **7** bound to the ATP-binding pocket of the PI3K α kinase catalytic domain and the conformation of **7** with PI3K α was similar to that of the PI3K α -**9d**. In detail, the morpholine moiety of **7** was in close proximity to the hinge region of the kinase with the oxygen, forming a hydrogen bond to amide of V851 and the carbon atoms packing against the side chain of V850 and M922 (Figure 3B). The hydrophobic thienopyrimidine core of the compound packed against the side chain of M772, W780, I932, and I800. The phenol moiety pointed toward a pocket formed by residues Y836, D810, I848, and I932. Two hydrogen bonds were formed between the hydroxyl group of the phenol moiety and the Asp810 carboxyl side chain and Tyr836 hydroxyl group. That explained why the hydroxyl was so critical for activity and precious attempts to replace the hydroxyl group on related templates resulted in a significant loss of activity. Finally, the amino group extended toward the sidechain of L807, D805, K802 and I848, forming a hydrogen bond to the amino of K802. Residue L807, D805, K802, and I848 formed a modest pocket, which may explain the sensitive activity to the chain length.

1.3. Selectivity of other isoforms of PI3Ks

To check selectivity for PI3K α , compound **7**, **20**, **21**, **22**, and **PI103** were evaluated against other PI3K isoforms (Table 3). **7** was equipotent against PI3K α and PI3K δ , while displaying about 3-fold selectivity for PI3K α over PI3K β and 6-fold selectivity for PI3K α over PI3K γ . **20** showed about 7-fold selectivity for PI3K α over PI3K β and 5-fold selectivity for PI3K α over PI3K γ and PI3K δ . **21** exhibited about 13-fold selectivity for PI3K α over PI3K γ and 4-fold selectivity for PI3K α over PI3K β and PI3K δ . **22** showed about 18-fold selectivity for PI3K α over PI3K β and 6-fold more selectivity for PI3K α over PI3K γ and PI3K δ . **7** and **21** were promising dual PI3K α/δ inhibitors. **20** and **22** were PI3K α inhibitors with modest isoform selectivity. Since mTOR and PI3K conserved a typical ATP site despite their little kinase fold resemblance, we also evaluated the inhibitory effect of our compounds on mTOR. As it turns out, **7**, **20**, **21**, and **22** also displayed good nanomolar inhibitions against mTOR. These experiments demonstrated that increasing the length of R₂ substituents could improve the selectivity for PI3K α but decrease the enzymatic activity of PI3K α .

1.4. Antiproliferative Activity in Selected Cell Lines

To investigate the functional consequence of inhibiting PI3K α in cells, three cell lines with *PIK3CA* activating mutations, SKOV3 ovarian cancer cell line (H1047R), Rh30 rhabdomyosarcoma cell line (high activation) and PC3 human prostate cancer cell line (PTEN deletion), were treated with **7**, **20**, **21**, **22** and growth was monitored. All these PI3K-activated cell lines were growth inhibited by exposure to compounds for 96h. As shown in Table 4, **7** and **21** potently inhibited the proliferation of all of the cell lines examined, irrespective of the different triggers for PI3K activation in these cell lines, with GI₅₀ values in the nanomolar range, which were lower than those obtained with PI103. However, **20** and **22** were less potent than PI103 in inhibiting cell proliferation. These results suggested that, **7** and **21**, represented lead compounds for further optimization of cancer therapy targeting class I PI3K.

1.5. **7** and **20** inhibits PI3K Signaling

Compounds **7** and **20** as PI3K α inhibitors potently blocked phosphorylation of Akt in SKOV3 ovarian cancer cell and Rh30 rhabdomyosarcoma cell (Figure 4). They also blocked activation of the mTORC1 pathway as measured by phosphorylation of the mTORC1 target 4E-BP1. This result indicated that **7** and **20** suppressed SKOV3 cell and Rh30 cell proliferation by inhibition of intracellular PI3K/AKT/mTOR pathway.

Conclusions

A series of thieno[3,2-d]pyrimidine derivatives was designed using the combination strategy based our previous potency compound **9d** and GDC-0941. The synthesis and biological evaluation of the derivatives demonstrated their nanomole enzymatic and cellular activities against PI3K with acceptable kinase selectivity, suggesting the successful of our combination strategy. Further determination of complex PI3K α -**7** provided accurate structural insights for their high-affinity interactions with PI3K α and a structural basis for further design and optimization. The simplified thieno[3,2-d]pyrimidine derivatives was potency PI3K α inhibitor with low molecular weight. A particular focus will be made on bioavailability evaluation and ADME-toxicity studies. Further optimization may ultimately yield a chemical series to progress into vivo experiments.

Acknowledgments

This work was funded by the National Basic Research Program of China (973 Program) (2015CB910403), the National Natural Science Foundation of China (81721004 to J.Z. and 21702137 to X.Y), and the Shanghai Sailing Program (17YF1410600 to X.Y).

Conflict of Interest

The authors have declared no conflict of interest.

Supplementary Material

Experimental section: Synthetic details, characterization data for all compounds.

NMR Spectrum: ^1H - and ^{13}C -NMR spectrum of new compounds **7**, **20-22**.

Figure legend

Figure 1. Structures of PI3K inhibitors undergoing clinical trials.

Figure 2. Design strategy of the thieno[3,2-d]pyrimidine derivatives based on **GDC-0941** and **9d**.

Figure 3. (A) X-ray complex of **7** (blue, sticks) to PI3K α (grey, surface, PDB ID: 5XGI). (B) The interactions between **7** (blue, sticks) and PI3K α (pink, carton). The key binding site residues of PI3K α are shown as sticks. Hydrogen bonds between **7** and the protein are shown as a red dashed line.

Figure 4. Inhibition of PI3K-mediated signaling by test compounds in SKOV3 and Rh30 cells. SKOV3 cells were incubated with test compounds at the desired concentrations for 1 h. Cells were collected for Western blot to analyze the level of phosphorylated AKT at S473 and 4E-BP1. Representative images of three independent experiments are shown.

References

1. A. Arcaro, A. S. Guerreiro, *Current Genomics* **2007**, 8, 271-306.
2. D. Gyori, T. Chessa, P. T. Hawkins, L. R. Stephens, *Cancer* **2017**, 9, 24.
3. D. A. Sabbah, J. Hu, H. A. Zhong, *Current Topics in Medicinal Chemistry* **2016**, 16, 1413-1426.
4. P. Chen, L. Zhang, J. M. Ding, J. Zhu, Y. Li, S. G. Duan, H. T. Yan, Y. W. Huan, J. H. Dong, *Biochemical and Biophysical Research Communications* **2006**, 342, 887-893.
5. J. A. Engelman, *Cancer* **2009**, 9, 550-562.
6. P. Liu, H. Cheng, T. M. Roberts, J. J. Zhao, *Nature Reviews Drug Discovery* **2009**, 8, 627-644.
7. V. Ludovini, F. Bianconi, L. Pistola, R. Chiari, V. Minotti, R. Colella, D. Giuffrida, F. R. Tofanetti, A. Siggillino, A. Flacco, E. Baldelli, D. Iacono, M. G. Mameli, A. Cavaliere, L. Crino, *Journal of Thoracic Oncology* **2011**, 6, 707-615.
8. S. J. Rogers, C. Box, K. J. Harrington, C. Nutting, P. Rhys-Evans, S. A. Eccles, *Expert Opinion on Therapeutic Targets* **2005**, 9, 769-790.
9. W. A. Denny, *Expert Opinion on Therapeutic Patents* **2013**, 23, 789-799.
10. Z. Zheng, S. I. Amran, J. Zhu, O. Schmidt-Kittler, K. W. Kinzler, B. Vogelstein, P. R. Shepherd, P. E. Thompson, I. G. Jennings, *The Biochemical Journal* **2012**, 444, 529-535.

11. J. R. Garlich, P. De, N. Dey, J. D. Su, X. Peng, A. Miller, R. Murali, Y. Lu, G. B. Mills, V. Kundra, H. K. Shu, Q. Peng, D. L. Durden, *Cancer Research* **2008**, 68, 206-215.
12. L. C. Foukas, I. M. Berenjano, A. Gray, A. Khwaja, B. Vanhaesebroeck, *Proceedings of the National Academy of Sciences of the United States of America* **2010**, 107, 11381-11386.
13. C. E. Edling, F. Selvaggi, R. Buus, T. Maffucci, P. Di Sebastiano, H. Friess, P. Innocenti, H. M. Kocher, M. Falasca, *Clinical Cancer Research* **2010**, 16, 4928-4937.
14. G. A. Morales, J. R. Garlich, J. Su, X. Peng, J. Newblom, K. Weber, D. L. Durden, *Journal of Medicinal Chemistry* **2013**, 56, 1922-1939.
15. T. P. Heffron, L. Salphati, B. Alicke, J. Cheong, J. Dotson, K. Edgar, R. Goldsmith, S. E. Gould, L. B. Lee, J. D. Lesnick, C. Lewis, C. Ndubaku, J. Nonomiya, A. G. Olivero, J. Pang, E. G. Plise, S. Sideris, S. Trapp, J. Wallin, L. Wang, X. Zhang, *Journal of Medicinal Chemistry* **2012**, 55, 8007-8020.
16. Y. Samuels, Z. Wang, A. Bardelli, N. Silliman, J. Ptak, S. Szabo, H. Yan, A. Gazdar, S. M. Powell, G. J. Riggins, J. K. Willson, S. Markowitz, K. W. Kinzler, B. Vogelstein, V. E. Velculescu, *Science* **2004**, 304, 554.
17. S. Velho, C. Oliveira, A. Ferreira, A. C. Ferreira, G. Suriano, J.S. Schwartz, A. Duval, F. Carneiro, J. C. Machado, R. Hamelin, R. Seruca, *European Journal of Cancer* **2005**, 41, 1649-1654.
18. D. A. Fruman, C. Rommel, *Cancer Discovery* **2011**, 1, 562-572.
19. M. Hayakawa, H. Kaizawa, H. Moritomo, T. Koizumi, T. Ohishi, M. Yamano, M. Okada, M. Ohta, S. Tsukamoto, F. I. Raynaud, P. Workman, M. D. Waterfield, P. Parker, *Bioorganic & Medicinal Chemistry Letters* **2007**, 17, 2438-2442.
20. Y. Zhao, X. Zhang, Y. Chen, S. Lu, Y. Peng, X. Wang, C. Guo, A. Zhou, J. Zhang, Y. Luo, Q. Shen, J. Ding, L. Meng, J. Zhang, *ACS Medicinal Chemistry Letters* **2014**, 5, 138-142.
21. M. Hayakawa, H. Kaizawa, H. Moritomo, T. Koizumi, T. Ohishi, M. Okada, M. Ohta, S. Tsukamoto, P. Parker, P. Workman, M. Waterfield, *Bioorganic & Medicinal Chemistry* **2006**, 14, 6847-6858.
22. M. Nacht, L. Qiao, M. P. Sheets, T. St Martin, M. Labenski, H. Mazdiyasi, R. Karp, Z. Zhu, P. Chaturvedi, D. Bhavsar, D. Niu, W. Westlin, R. C. Petter, A. P. Medikonda, J. Singh, *Journal of Medicinal Chemistry* **2013**, 56, 712-721.
23. N. Srimongkolpithak, S. Sundriyal, F. L. Li, M. Vedadi, M. J. Fuchter, *Medicinal Chemistry Communication* **2014**, 5, 1821-1828.
24. W. F. Zhu, C. Chen, C. Y. Sun, S. Xu, C. J. Wu, F. Lei, H. Xia, Q. D. Tu, P. W. Zheng, *European Journal of Medicinal Chemistry* **2015**, 93, 64-73.
25. J. Li, L. Sun, C. Xu, F. Yu, H. Zhou, Y. Zhao, J. Zhang, J. Cai, C. Mao, L. Tang, Y. Xu, J. He, *Acta Biochimica et Biophysica Sinica* **2012**, 44, 300-306.
26. S. Chen, T. Hu, J. Zhang, J. Chen, K. Chen, J. Ding, H. Jiang, X. Shen, *The Journal of Biological Chemistry* **2008**, 283, 554-564.
27. S. Lu, A. Banerjee, H. Jang, J. Zhang, V. Gaponenko, R. Nussinov, *The Journal of Biological Chemistry* **2015**, 290, 28887-28900.
28. W. Huang, G. Wang, Q. Shen, X. Liu, S. Lu, L. Geng, Z. Huang, J. Zhang, *Bioinformatics* **2015**, 31, 2598-600.
29. C. Han, J. Zhang, L. Chen, K. Chen, X. Shen, H. Jiang, *Bioorganic & Medicinal Chemistry Letters* **2007**, 15, 656-662.
30. J. Li, J. Zhang, J. Chen, X. Luo, W. Zhu, J. Shen, H. Liu, X. Shen, H. Jiang, *Journal of Combinatorial Chemistry* **2006**, 8, 326-337.
31. H. Jiang, R. Deng, X. Yang, J. Shang, S. Lu, Y. Zhao, K. Song, X. Liu, Q. Zhang, Y. Chen, Y. E. Chinn, G. Wu,

J. Li, G. Chen, J. Yu, J. Zhang, *Nature Chemical Biology* **2017**, 13, 994-1001.

32. Q. Shen, F. Cheng, H. Song, W. Lu, J. Zhao, X. An, M. Liu, G. Chen, Z. Zhao, J. Zhang, *The American Journal of Human Genetics* **2017**, 100, 5-20.

33. C. Han, J. Zhang, L. Chen, K. Chen, X. Shen, H. Jiang, *Bioorganic & Medicinal Chemistry* **2007**, 15, 656-662.

34. X. Hou, J. Du, J. Zhang, L. Du, H. Fang, M. Li, *Journal of Chemical Information and Modeling* **2013**, 53, 188-200.

35. X.Y. Yng, X. Zhang, M. Huang, K. Song, X. F. Li, M. L. Meng, J. Zhang, *Scientific Reports* **2017**, 7, 14572.

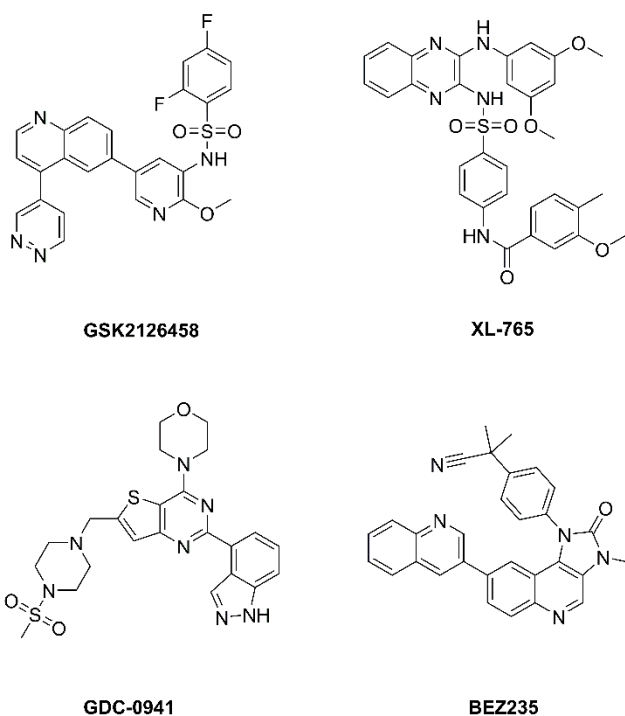


Figure 1. Structures of PI3K inhibitors undergoing clinical trials.

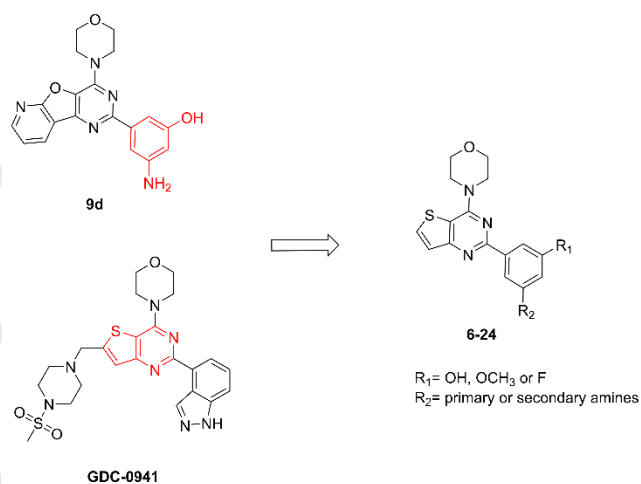


Figure 2. Design strategy of the thieno[3,2-d]pyrimidine derivatives based on **GDC-0941** and **9d**.

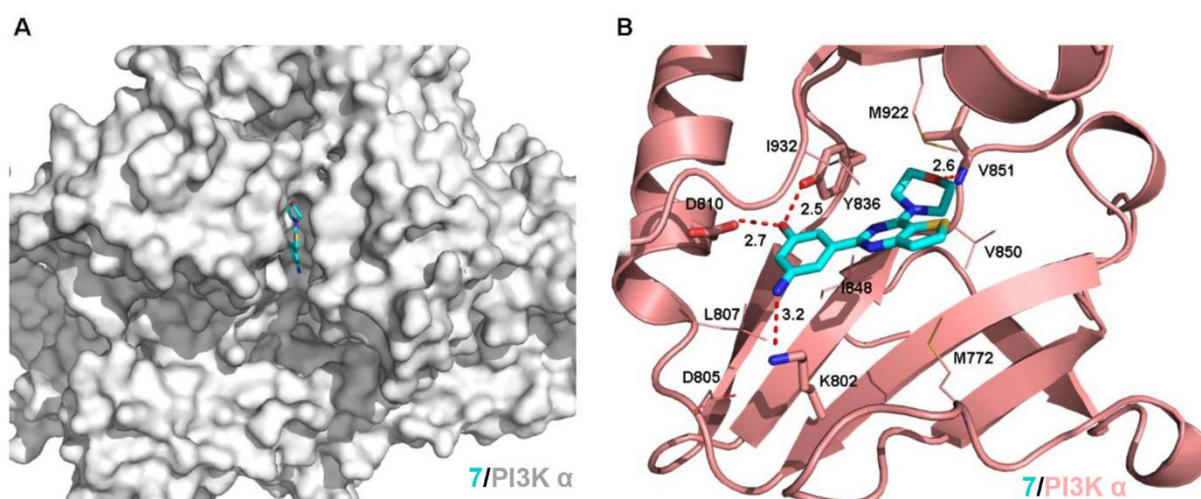


Figure 3. (A) X-ray complex of **7** (blue, sticks) to PI3K α (grey, surface, PDB ID: 5XGI). (B) The interactions between **7** (blue, sticks) and PI3K α (pink, carton). The key binding site residues of PI3K α are shown as sticks. Hydrogen bonds between **7** and the protein are shown as a red dashed line.

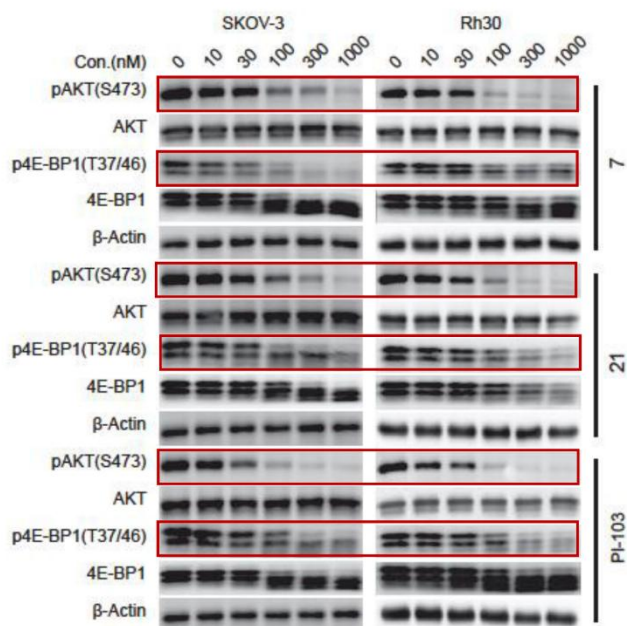
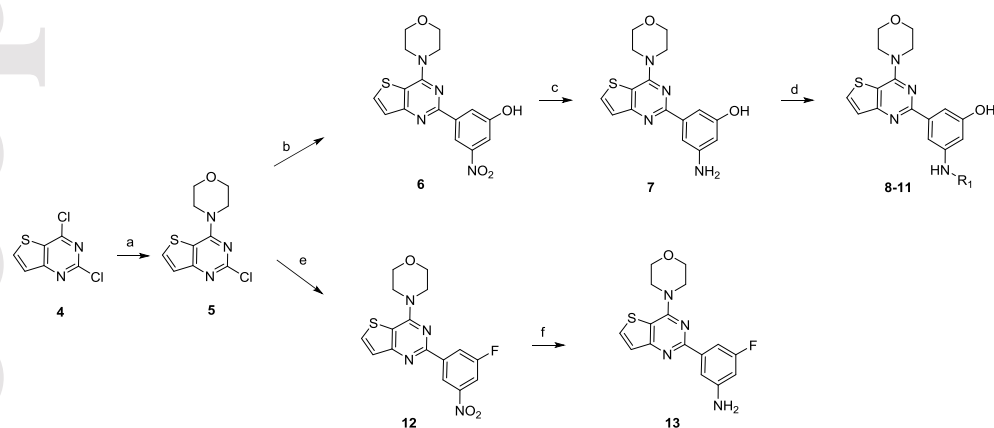


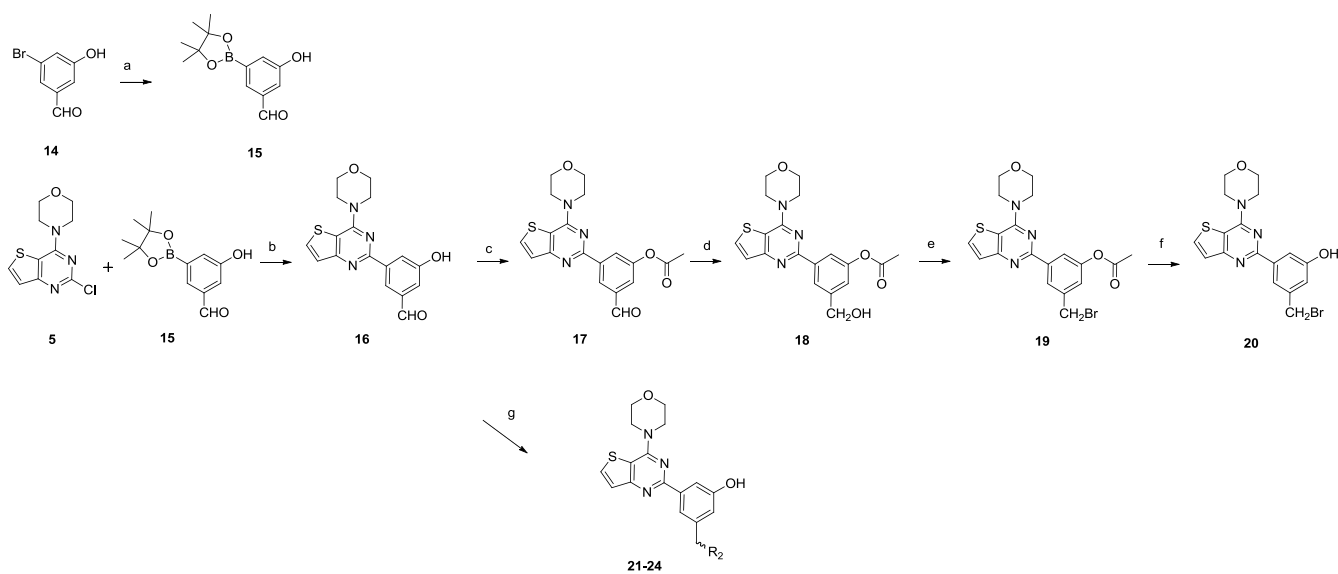
Figure 4. Inhibition of PI3K-mediated signaling by test compounds in SKOV3 and Rh30 cells. SKOV3 cells were incubated with test compounds at the desired concentrations for 1 h. Cells were collected for Western blot to analyze the level of phosphorylated AKT at S473 and 4E-BP1. Representative images of three independent experiments are shown.

Scheme 1^a

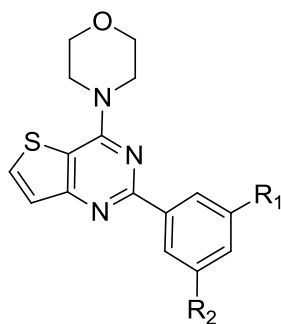


^a Reagents and conditions: (a) Morpholine, MeOH; (b) (3-hydroxy-5-nitrophenyl)boronic acid, Pd(PPh₃)₄, K₂CO₃; (c) Fe, NH₄Cl, EtOH; (d) Sodium triacetoxyborohydride, THF; (e) (3-fluoro-5-nitrophenyl)boronic acid, Pd(PPh₃)₄, K₂CO₃; (f) Fe, NH₄Cl, EtOH.

Scheme 2^a



^a Reagents and conditions: (a) Bis(pinacolato)diboron, Pd(dppf)Cl₂, K₂CO₃; (b) Pd(PPh₃)₄, K₂CO₃; (c) CH₃COCl, CH₂Cl₂; (d) NaBH₄, THF; (e) NBS, PPh₃; (f) 1N NaOH, MeOH; (g) 21: Sodium triacetoxyborohydride, THF; 22: Hydroxylamine hydrochloride, THF; 23: Malonic acid, toluene; 24: Hydrazine hydrate, THF.

Table 1. Kinase Inhibition against PI3K α 

Compound	R ₁	R ₂	PI3K α IC ₅₀ ^a (nM)
6	OH	NO ₂	2723.5 ± 860.5
7	OH	NH ₂	31.6 ± 9.4
8	OH		998.6 ± 170.3
9	OH		1643.5 ± 357.1
10	OH		4112.5 ± 794.1
11	OH		> 10,000
13	F	NH ₂	6301 ± 108.9
16	OH	CHO	> 1,000
19	OAc	CH ₂ Br	> 1,000
20	OH	CH ₂ Br	61.9 ± 1.1
21	OH	CH ₂ OH	12.5 ± 2.8
22	OH		59.2 ± 9.0
23	OH		> 1000
24	OH		> 1000
PI-103			17.0 ± 2.2

^aIC₅₀ values shown are the average of least two independent experiments in duplicate with typical variations of less than 20%.

Table 2. Data collection and Refinement Statistic for the Crystal Structure

PDB ID code	PI3K/7, 5XGI		
Data Collection			
Resolution (Å)*	50–2.56 (2.65–2.56)	γ (°)	90.00
Space group	P212121	Total reflections	310146
Cell dimensions		Unique reflections	47786
a (Å)	71.348	Completeness (%)*	99.8 (99.7)
b (Å)	135.825	Multiplicity*	6.5 (6.2)
c (Å)	150.245	Average I/ σ (I)*	12.7(2.2)
α (°)	90.00	Rmerge (%)*	14.4 (97.8)
β (°)	90.00		
Refinement			
Rwork (%)	23.9	Average B Value (Å ²)	77.083
Rfree (%)	29.0	Protein Mean B Value (Å ²)	77.261
RMSD in Bond Lengths (Å)	0.007	Ligand Mean B Value (Å ²)	49.368
RMSD in Bond Angles (°)	1.036	Water Mean B Value (Å ²)	55.038
Number of Atoms		Ramachandran Statistics	
Total	10818	Most favored regions	91.9%
Protein	10647	Additional allowed regions	8.0%
Ligand	23	Generously allowed regions	0.1%
Water	102	Disallowed regions	0.0%
B factor Statistics			

* Values in parentheses are for highest-resolution shell.

Table 3. Biochemical Selectivity of Compound 7, 20, 21, and 22 ^a

Compounds	IC ₅₀ (nM) ^b				
	PI3K α	PI3K β	PI3K γ	PI3K δ	mTOR
PI-103	17.0±2.2	173.3±50.6	571.4±133.4	215.0±101.9	27.1±1.4
7	31.6±9.4	101.5±26.9	243.3±81.8	33.4±3.8	21.6±6.0
20	61.9±1.1	428.1±50.8	297.8±8.6	344.6±80.1	57.5±16.6
21	12.5±2.8	70.2±12.5	276.3±151.8	47.2±7.5	12.5±3.8
22	59.2±9.0	1082.0±295.6	654.5±52.5	365.0±105.5	68.2±15.7

^a Effects of test compounds on the kinase activity of class I PI3K and mTOR were assessed as described in the Experimental Section.

^b IC₅₀ values shown are the average of least two independent experiments in duplicate with typical variations of less than 20%.

Table 4. The test compounds 7, 20, 21, and 22 inhibit proliferation of cancer cell ^a

Cell line	Cancer type	Genetic mutation	Proliferation IC ₅₀ ^b (μ M)				
			PI103	7	20	21	22
PC-3	Prostate	PTEN deletion	0.45±0.29	0.29±0.04	0.83±0.08	0.21±0.02	0.96±0.09
Rh30	Rhabdomyosarcoma	High activation	0.55±0.31	0.24±0.01	0.72±0.10	0.26±0.02	0.86±0.07
SKOV-3	Ovary cancer cells	PI3KCA mutation	0.27±0.17	0.11±0.01	0.38±0.08	0.15±0.01	0.33±0.04

^a Cell proliferation was assessed by an SRB assay as described in the Experimental Section. ^b IC₅₀ values shown are the average \pm SD of at least three independent experiments performed in triplicate.

Graphical Abstract

